



A Blind Cloud/Shadow Removal Strategy for Multi-Temporal Remote Sensing Images

Jie Lin¹,

Ting-Zhu Huang¹, Xi-Le Zhao¹, Meng Ding¹, Yong Chen², Tai-Xiang Jiang³

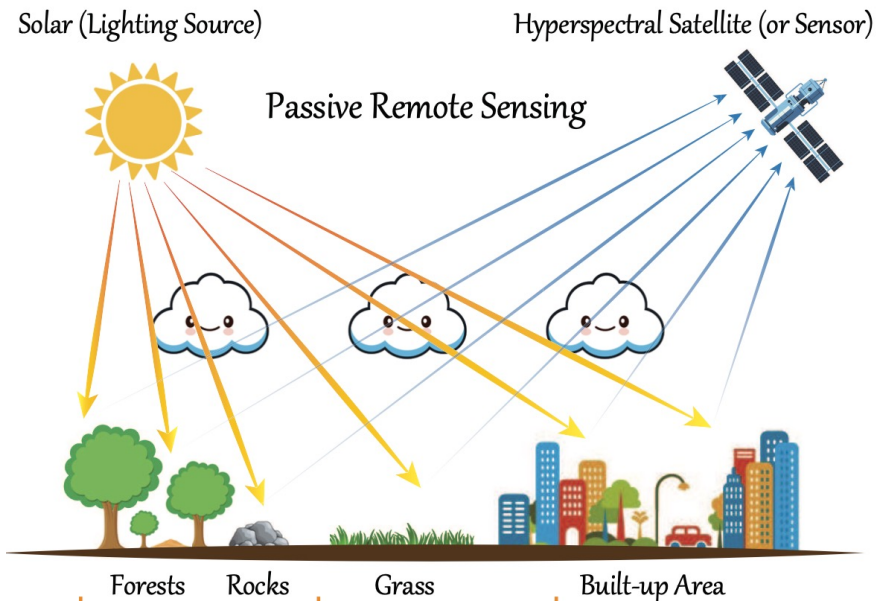
1. University of Electronic Science and Technology of China, China
2. Jiangxi Normal University, China
3. Southwestern University of Finance and Economics, China

IGARSS 2021



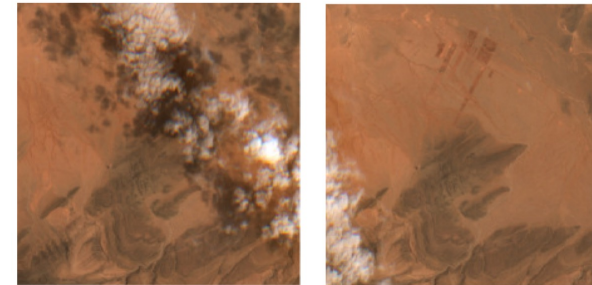
- Background
- Methodology
- Experiment
- Conclusion

➤ Imaging Process¹

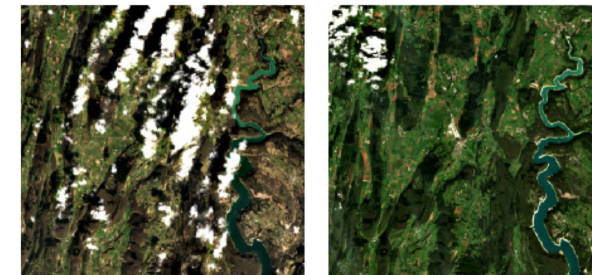


➤ Observed Remote Sensing (RS) Images

Sentinel-2 MSI

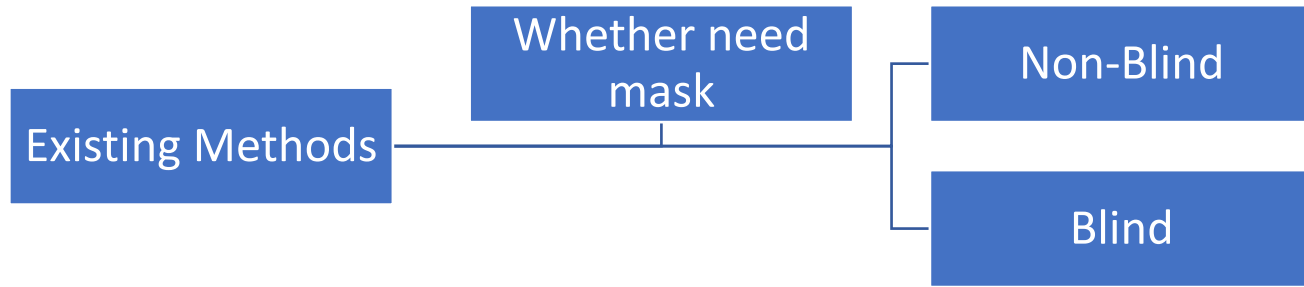


Landsat-8 MSI

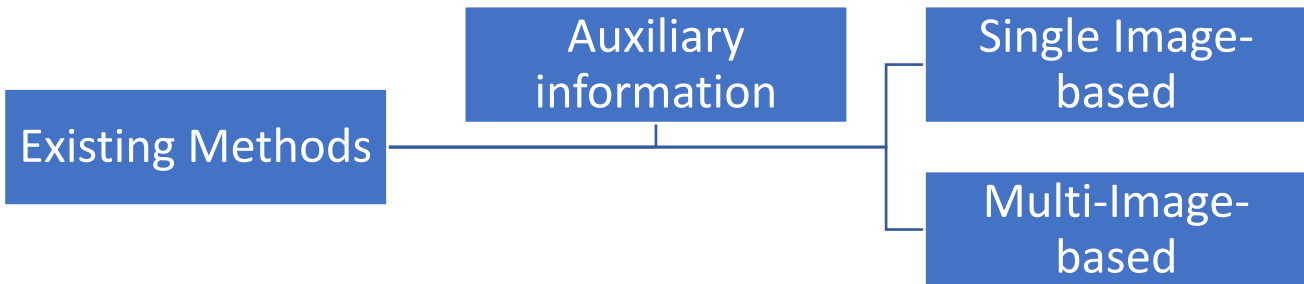


[1] D. Hong *et al.*, "Interpretable Hyperspectral Artificial Intelligence: When nonconvex modeling meets hyperspectral remote sensing," *IEEE Geoscience and Remote Sensing Magazine*, doi: 10.1109/MGRS.2021.3064051.

➤ Existing Thick Cloud Removal Methods



- Can achieve a more ideal cloud removal when the mask is inaccurate



- Can handle the large thick cloud contamination

- Background
- Methodology
- Experiment
- Conclusion

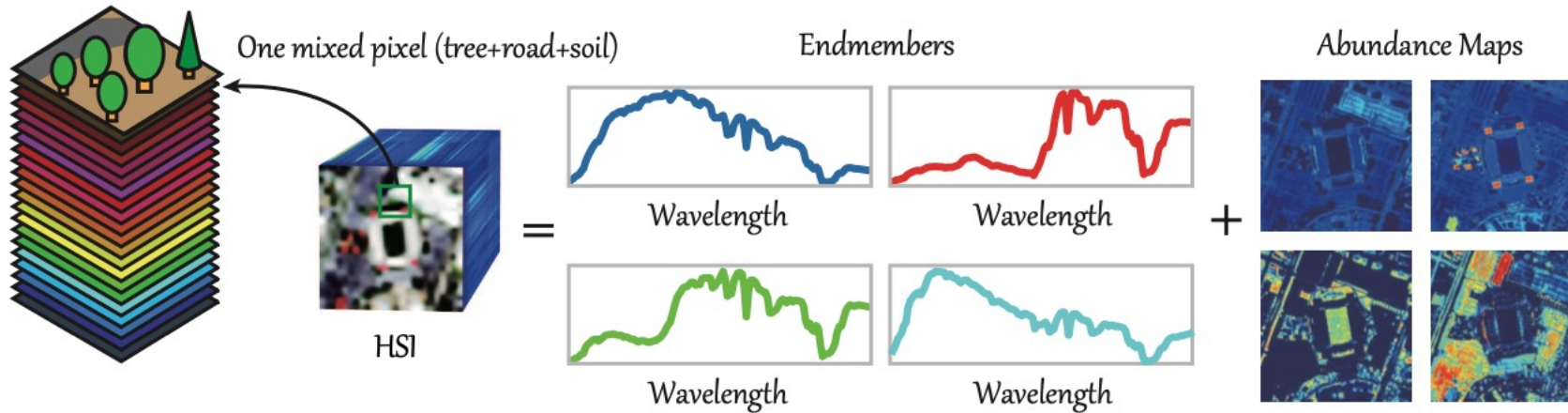
- **Aim:** Thick cloud removal for remote sensing image

Blind + Multi-Image-based method

- **Question**

- How to reduce the higher computational complexity due to the introduction of more auxiliary images?
- Is there any latent relationships between the multi-temporal RS images, which can be exploited to finely reconstruct the multi-temporal information?

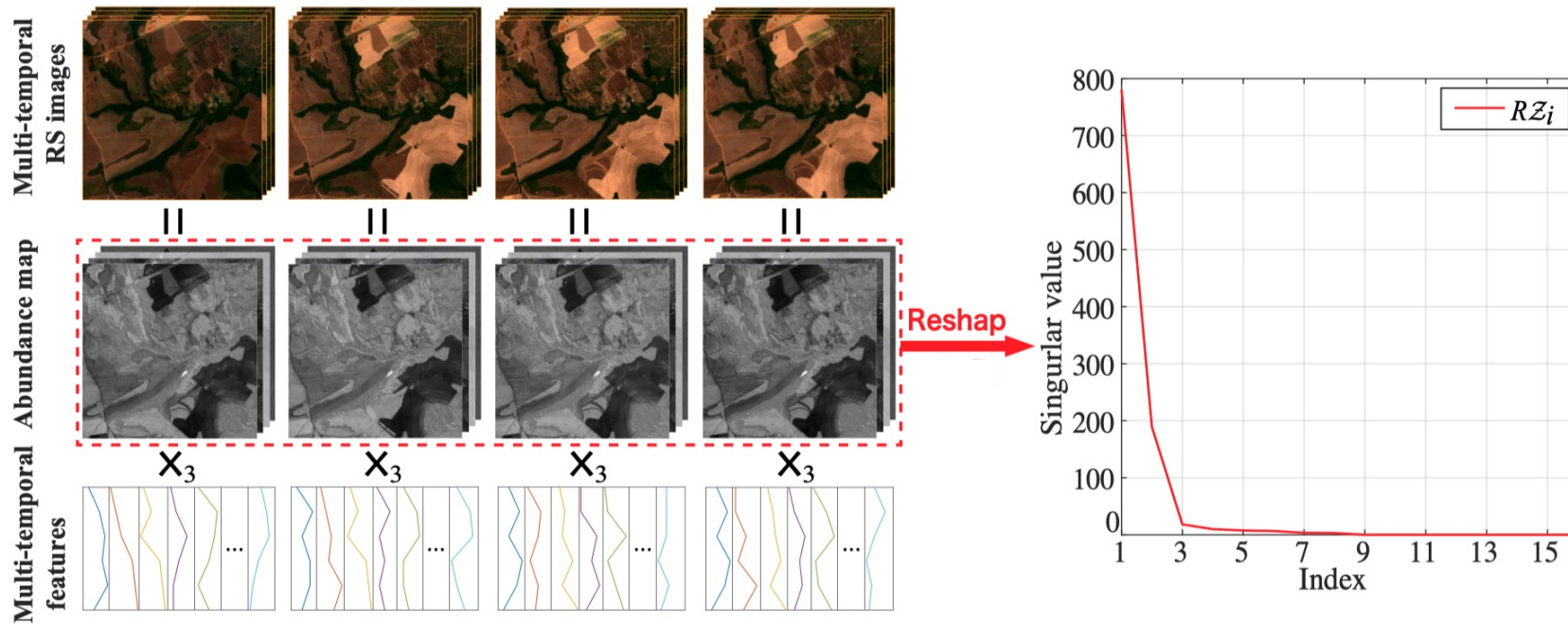
➤ Inspiration^[1]



Inspired by unmixing , as the distribution of surface material is constant over a period and the same material shows different spectral signatures at different time nodes, **the multi-temporal images in the same scene share the same abundances.**

[1] D. Hong *et al.*, "Interpretable Hyperspectral Artificial Intelligence: When nonconvex modeling meets hyperspectral remote sensing," in *IEEE Geoscience and Remote Sensing Magazine*, doi: 10.1109/MGRS.2021.3064051.

➤ Key Observation



Then, we use a coupled tensor factorization to explore this relationship, which decomposes the image at each time node into an abundance tensor that implies material distribution and orthogonal endmembers. **There is a strong similarity between abundance tensors over a period.**

➤ Proposed Method

- Degradation model

$$\mathcal{Y}_i = \mathcal{X}_i + \mathcal{C}_i + \mathcal{E}_i,$$

- Decomposition model

$$\mathcal{X}_i = \mathcal{A}_i \times_3 \mathbf{F}_i,$$

- Proposed Model

$$\min_{\mathcal{X}_i, \mathcal{C}_i, \mathcal{A}_i, \mathbf{F}_i} \sum_i \left\{ \frac{1}{2} \|\mathcal{Y}_i - \mathcal{C}_i - \mathcal{X}_i\|_F^2 + \beta \|\mathcal{C}_i\|_1 \right\} + \alpha \|\mathcal{R} \mathcal{A}_i\|_*,$$

$$\text{s.t. } \mathcal{X}_i = \mathcal{A}_i \times_3 \mathbf{F}_i, \mathbf{F}_i^T \mathbf{F}_i = \mathbf{I}, (\mathcal{X}_i)_{\bar{\Omega}} = (\mathcal{Y}_i)_{\bar{\Omega}}.$$

- Developed ALM algorithm

Algorithm 1 ALM-based Algorithm for the Proposed Model

Input: Observed RS images and Reference RS images $\{\mathcal{Y}_i\}$.

- 1: Initialize: $\mathcal{X}_i = \mathcal{Y}_i$, $\mathcal{C}_i = \mathcal{P}_i = \mathcal{O}$, and $\mathbf{W}_i = \mathbf{Q}_i = \mathbf{0}$.
- 2: **while** not converged **do**
- 3: Update $\{\mathbf{F}_i\}$, $\{\mathcal{A}_i\}$ by (4) and (5);
- 4: Update \mathbf{W} , $\{\mathcal{C}_i\}$, $\{\mathcal{X}_i\}$ by (6), (7), and (8);
- 5: Update $\{\mathcal{P}_i\}$ and \mathbf{Q} by (9);
- 6: Refine mask Ω by Algorithm 2.
- 7: **end while**

Output: Estimated RS images $\{\mathcal{X}_i\}$.

➤ Proposed Method

- Mask refinement strategy

Algorithm 2 Cloud/Shadow Detection

Input: Sparse component \mathcal{C}_i , threshold ϵ .

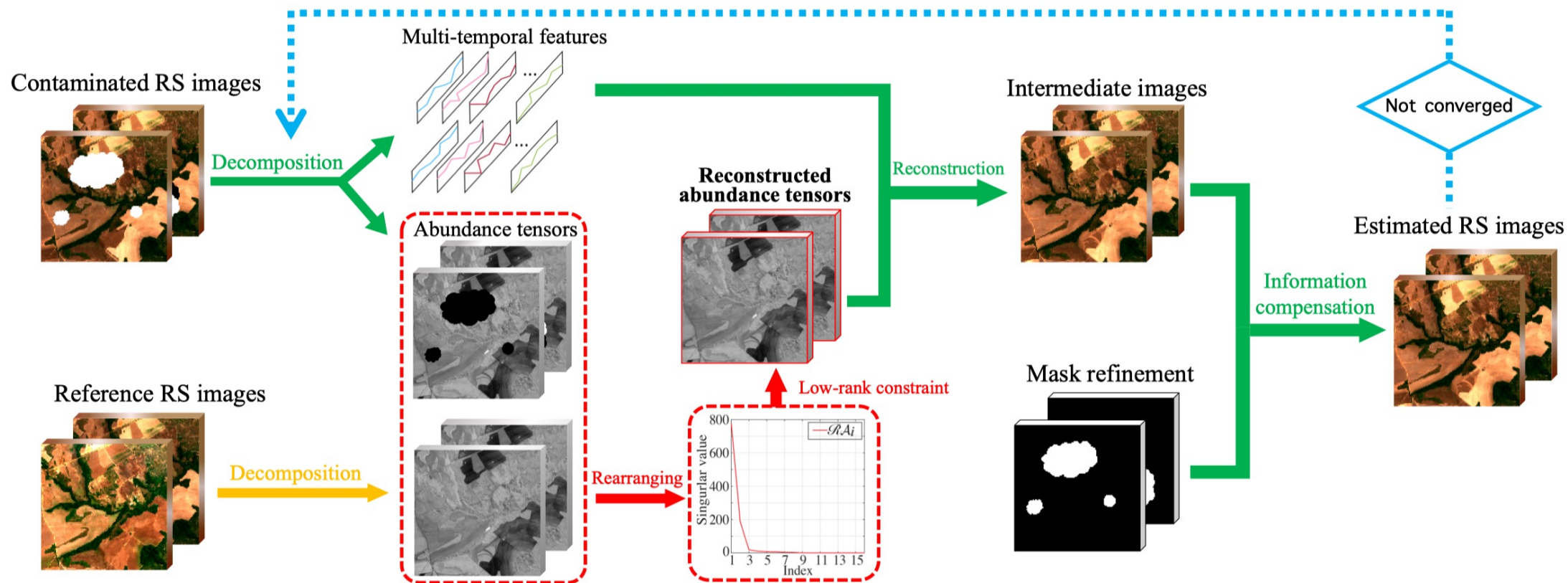
- 1: Initialize: $\Omega = \emptyset$.
- 2: **for** $p_1 = 1 : m$ **do**
- 3: **for** $p_2 = 1 : n$ **do**
- 4: Compute $a = \text{mean}(\mathcal{C}_i(p_1, p_2, :))$;
- 5: $\Omega = \Omega \cup (p_1, p_2, :)$, if $|a| > \epsilon$;
- 6: **end for**
- 7: **end for**

Output: The location of the cloud/shadow Ω .

We **embed the cloud/shadow detection (Algorithm 2)** in each iteration of **Algorithm 1** to refine the mask. The refined mask will help to introduce true information from observed images for multi-temporal feature learning.

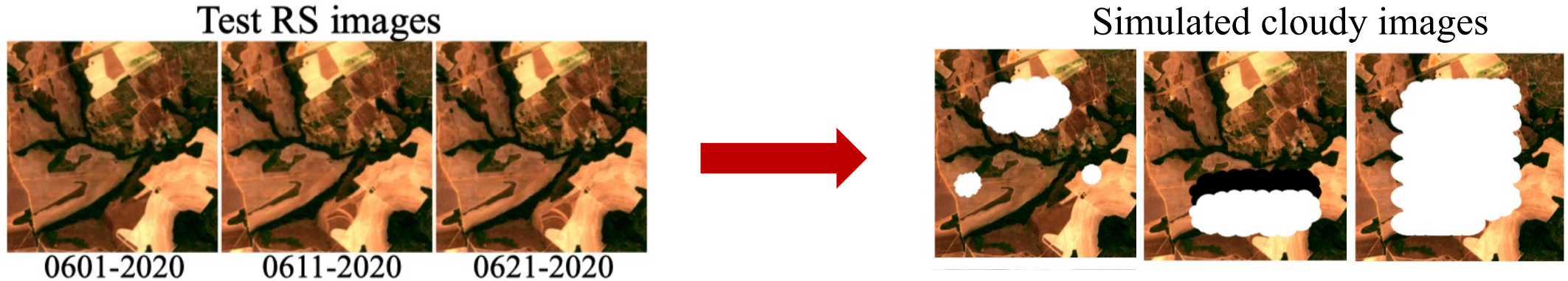
➤ Proposed Method

- Flowchart of the Proposed Method



- Background
- Methodology
- Experiment
- Conclusion

- Dataset: Brazil Dataset^[2]



This dataset is taken over Brazil by **Sentinel-2** and each temporal data contains four spectral bands (B2, B3, B4, and B8). The sub-images of size 400×400 of 6 different temporal data are used in our experiments.

- Comparison methods

Non-Blind temporal-based methods: ALM-IPG and WLR

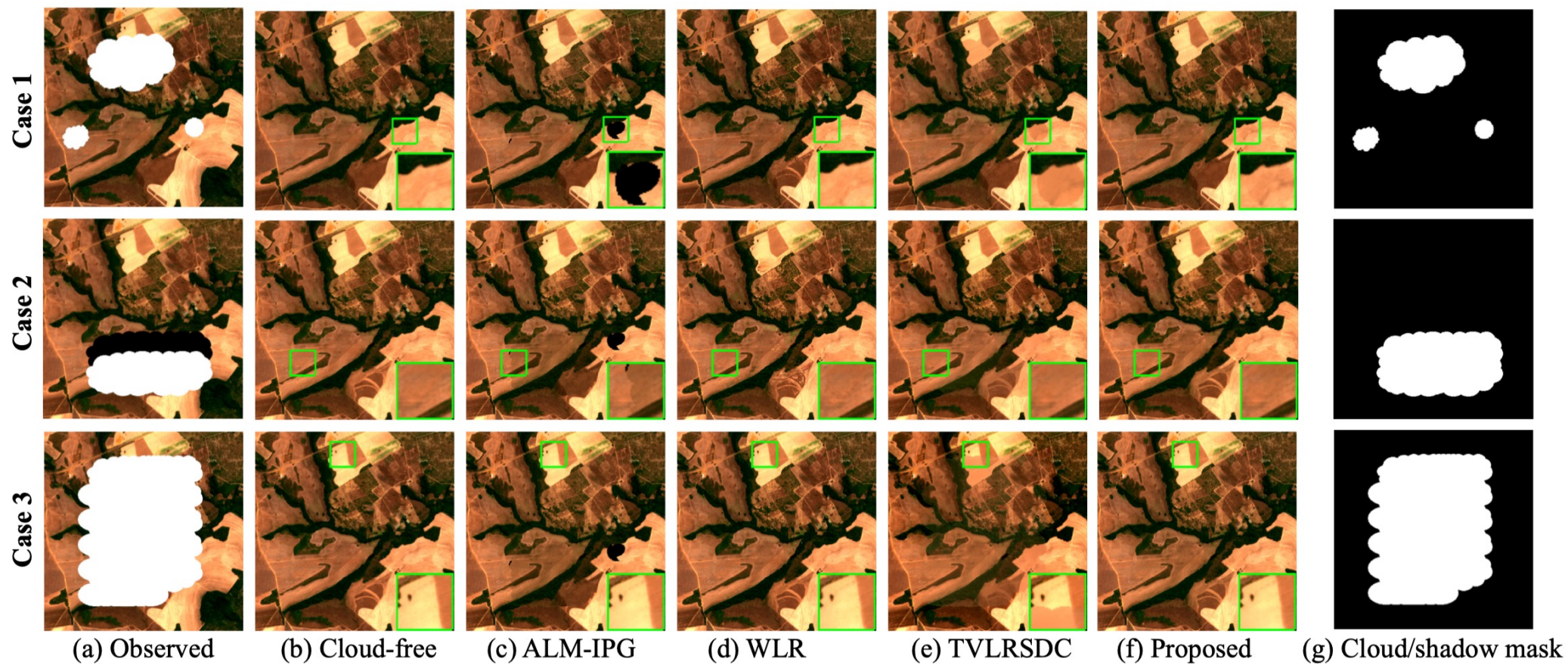
Blind temporal-based method: TVLRSDC

[2] <https://theia.cnes.fr/atdistrib/rocket/#/home>

- Index Evaluation

Case	Index	Observed	ALM-IPG	WLR	TVLRSDC	Proposed
Case 1	PSNR	11.921	32.164	41.420	40.578	49.264
	SSIM	0.8500	0.9840	0.9884	0.9947	0.9987
	CC	0.4905	0.9202	0.9901	0.9940	0.9987
Case 2	PSNR	11.543	30.923	37.336	40.790	49.154
	SSIM	0.7955	0.9703	0.9714	0.9901	0.9982
	CC	0.4512	0.8959	0.9750	0.9902	0.9982
Case 3	PSNR	6.2239	31.168	42.735	36.780	44.670
	SSIM	0.5580	0.9669	0.9933	0.9664	0.9952
	CC	0.1728	0.9010	0.9943	0.9542	0.9956
Time		—	0.7528	2.0179	4.8299	1.0934

- Visual Evaluation



- Background
- Methodology
- Experiment
- Conclusion

- **Key Observation:** There is a strong similarity between the abundance tensors at different times since the material distribution is constant to time in multi-temporal RS images.

- **Contribution:**
 - Based on our key observation, we suggest a cloud/shadow removal model, which faithfully reconstructs the underlying multi-temporal information through reconstructing abundance tensors and learning multi-temporal features.

 - We design a refinement strategy to refine the detected cloud/shadow mask, which helps to learn more accurate multi-temporal features.

Thanks!

Jie Lin

University of Electronic Science and Technology of China